applied sciences

MDPI

Article

A Design Method and Application of Backfilling Hydraulic Supports in Reforming Top-Coal Caving Hydraulic Supports

Qiang Zhang [1,2], Peitao Shi [1,2,*], Meng Li [1,2], Tingcheng Zong [1,2] and Weijian Song [1,2]

[1] School of Mines, China University of Mining & Technology, Xuzhou 221116, China
[2] Key Laboratory of Deep Coal Resource Mining, Ministry of Education of China, China University of Mining & Technology, Xuzhou 221116, China
* Correspondence: tb20020025b1@cumt.edu.cn

Abstract: Solid backfilling is an environmentally friendly method of coal mining. Backfilling hydraulic supports are important devices in solid backfill mining. In order to speed up the design and manufacturing process of them, this paper proposes a method of hydraulic support reformation and evaluation. The mechanical models of top-coal caving hydraulic support and backfilling hydraulic support were established to analyze the stress characteristics of the main structure. ABAQUS was used to establish the 3D numerical model to analyze the load-bearing characteristics, as well as verify the strength requirement. In addition, the structural characteristics, compaction characteristics, geological adaptation characteristics, and interference characteristics of the structure were analyzed using motion simulation. After reforming, the ramming force is just above 2.0 MPa, and the utilization ratio of the old parts of the top-coal caving hydraulic support is more than 50%, which saved the costs of the new backfilling hydraulic support and reduced the waste of idle top-coal caving hydraulic support. The successful application of the backfilling hydraulic support in the Tangshan mine showed the rationality of the reform design.

Keywords: hydraulic support reform; backfilling hydraulic support; stress analysis; motion simulation; finite element analysis

check for updates

Citation: Zhang, Q.; Shi, P.; Li, M.; Zong, T.; Song, W. A Design Method and Application of Backfilling Hydraulic Supports in Reforming Top-Coal Caving Hydraulic Supports. *Appl. Sci.* **2023**, *13*, 987. https://doi.org/10.3390/app13020987

Academic Editor: Raffaele Zinno

Received: 24 November 2022
Revised: 25 December 2022
Accepted: 27 December 2022
Published: 11 January 2023

Copyright: © 2023 by the authors. Licensee MDPI, Basel, Switzerland. This article is an open access article distributed under the terms and conditions of the Creative Commons Attribution (CC BY) license (https://creativecommons.org/licenses/by/4.0/).

1. Introduction

The caving method for coal mining may result in ecological damage [1,2], such as surface subsidence [3], water loss [4] and building damage [5]. Previous studies have shown that mining technologies that can protect the ecology mainly include hydraulic sand backfill [6], high-water backfill [7,8], paste backfill [9–11] and solid backfill [12,13]. The first three are in the form of slurry to pump the filling material into the goaf, which have been widely used in countries such as Germany [14], Russia [15], Turkey [16,17], Poland [18], and India [19–21]. The latter is to fill massive gangue and loess into goaf and squeeze them to support overlying strata, a method mainly used in China at present. The basic principle of solid backfill is shown in Figure 1. The transportation route of the solid backfilling material is as follows [22]: gangue dump and loess dump → vertical feeding shaft → surge bin → goaf (the blue route in Figure 1a). The scraper conveyor at the back of the backfilling hydraulic support (Figure 1b) in the working face puts the filling material into the goaf, and the tamping mechanism at the back of the backfilling hydraulic support (Figure 1b) squeezes the filling material. The higher the squeezing degree, the higher the backfilling rate [23,24], and the better the effect of supporting the overlying strata [5,25].

Previous studies have shown that backfilling hydraulic support is the core equipment of solid backfill [26,27]. On the one hand, enough support resistance can support the overlying strata and maintain the space of goaf [28]. On the other hand, the backfilling rate depends on the force of the tamping mechanism. Therefore, an efficient design and manufacturing process, as well as good operation performance, is the guarantee

of backfilling. The research shows that at present, the design method of backfill hydraulic support is mainly redesigned according to the weight of rock stratum, and there are few cases of transforming other hydraulic support into backfilling hydraulic support; so, the design and manufacturing cycle of backfilling hydraulic support is longer [29]. The main method to test the operation performance of backfilling hydraulic support is a physical test [30], as shown in Figure 2; the object of physical test is the prototype that has been manufactured, and its test cost is high and the test process is slow. Some scholars also use simulation to test the strength of shield hydraulic support [31,32], mainly simulating the strength of key components, such as columns and bases. Additionally, some scholars use the digital twin theory to test the virtual hydraulic support [33,34], but it is difficult to test the compressive strength of the hydraulic supports.

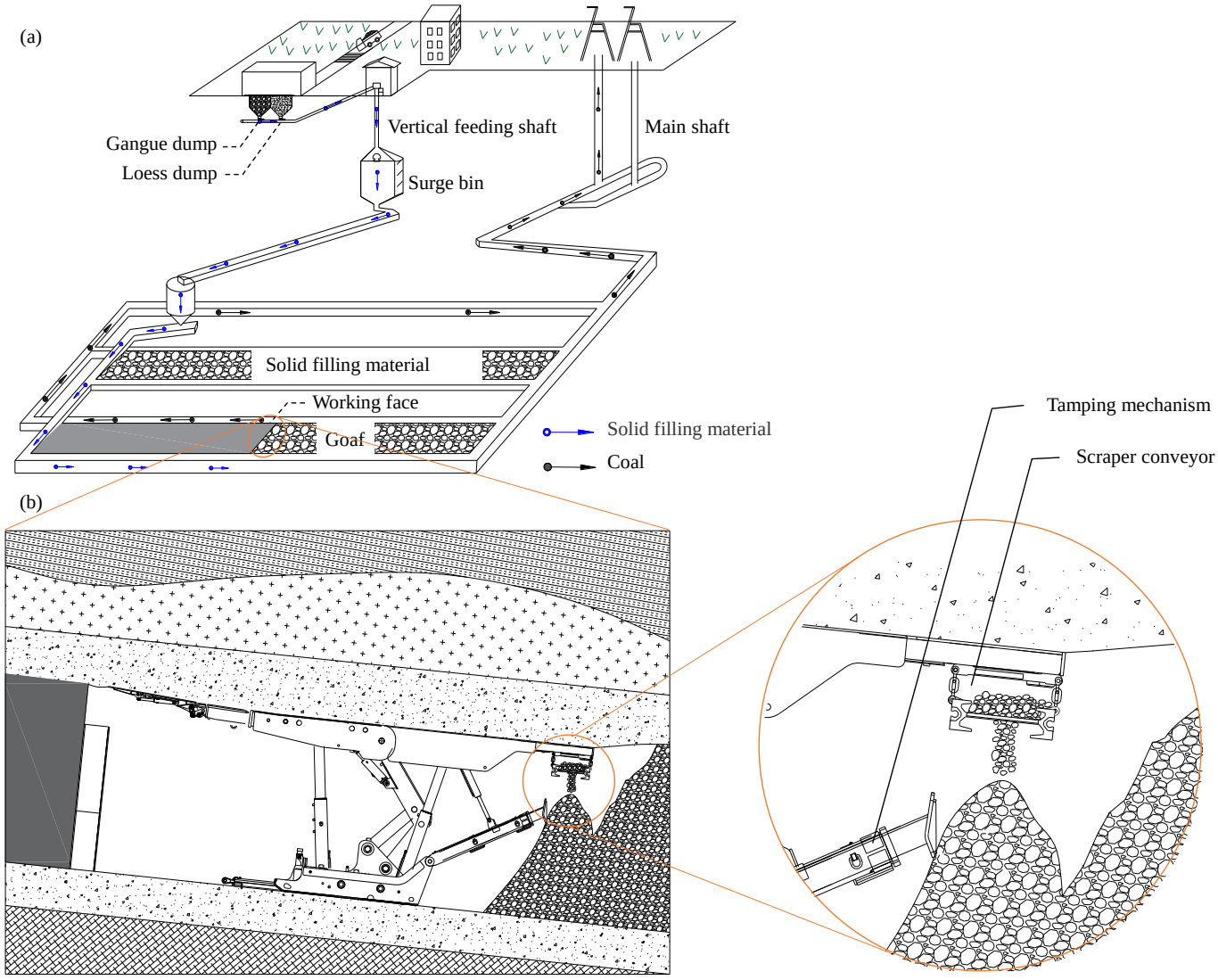


Figure 1. Basic principle of solid backfill mining: (**a**) transportation route; (**b**) basic principle of backfilling hydraulic support.

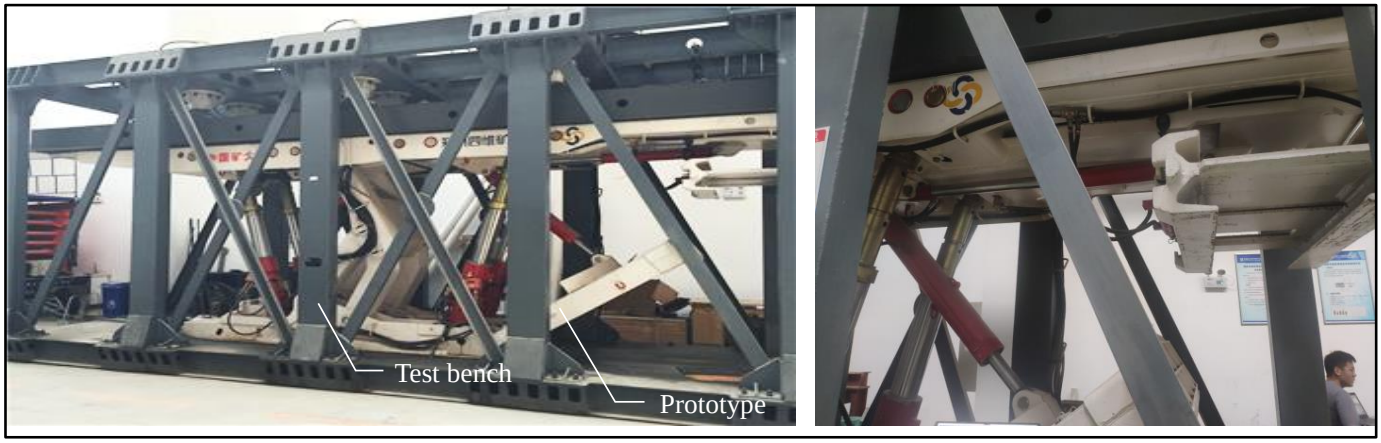


Figure 2. Prototype test of backfilling hydraulic support.

Through the above analysis, the following problems in the backfilling hydraulic support can be found: long design cycle and high manufacturing cost; the inspection method is mainly from the perspective of strength, and seldom considers the comprehensive influence of structure and strength. Therefore, this paper proposed the design method of transforming top-coal caving hydraulic support into backfilling hydraulic support. The paper calculated the bearing capacity of the top-coal caving hydraulic support and the backfilling hydraulic support theoretically. ABAQUS (6.14) was used to simulate the strength of the reformed backfilling hydraulic support, Creo was used to perform a simulation check of the structure. In addition, this paper demonstrates the feasibility of the reformation with field applications. The results of the study contribute to the efficient design and performance evaluation of the backfilling hydraulic support.

2. Materials

The object of reformation is the top-coal caving hydraulic support from Tangshan mine in China, which was originally used in the coal seam with an average thickness of 2.5 m; when mining below the city, however, the caving method could not be used for coal mining underground, so the top-coal caving hydraulic support was useless. Additionally, solid backfilling can realize safe coal mining under cities. Accordingly, this study proposed to transform the idle top-coal caving hydraulic support into backfilling hydraulic support. The main parameters of top-coal caving hydraulic support are shown in Figure 3 and Table 1.

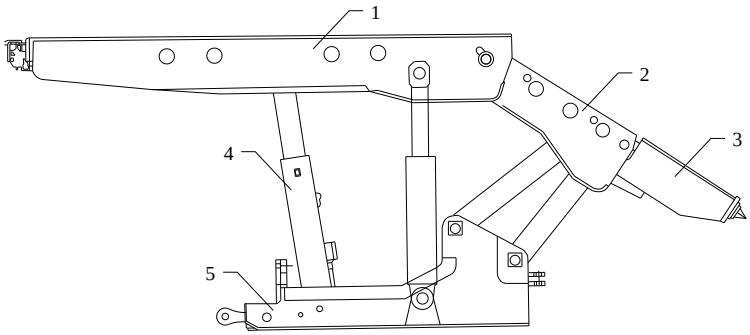


Figure 3. Plane structure of the ZFS5600/16/32 top-coal caving hydraulic support. 1. Top beam; 2. Shield beam; 3. Coal caving organization; 4. Column; 5. Base.

Table 1. The basic parameters of the ZFS5600/16/32 top-coal caving hydraulic support.

Objects	Parameters	Objects	Parameters
Height (mm)	1600~3200	Initial support force (kN)	5236
Width (mm)	1420~1290	Working resistance (kN)	5600
Center distance (mm)	1500	Floor specific pressure (MPa)	1.83

3. Design Method of Replacing Top-Coal Caving Hydraulic Supports with Backfilling Hydraulic Supports

3.1. Design Process of Support Reconstruction

Combined with the general principles of the hydraulic support design and the structure of the top-coal caving hydraulic support, the process of designing the top-coal caving hydraulic support to replace the backfilling hydraulic support is shown in Figure 4.

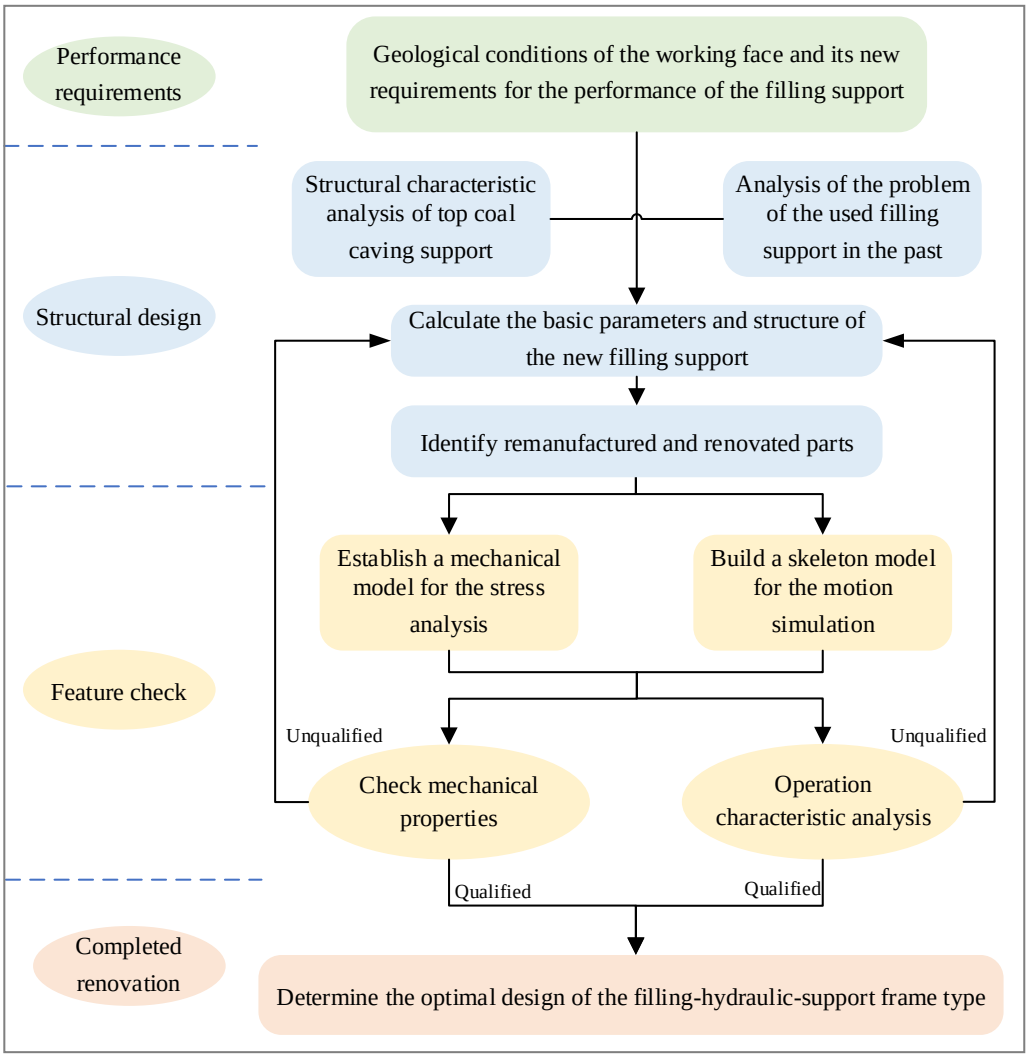


Figure 4. Design flow of refitting the backfilling hydraulic support in the top-coal caving hydraulic support.

The work specifically takes the reformation of the ZFS5600/16/32 top-coal caving hydraulic support into a new type of the backfilling hydraulic support as an example to describe the transformation design process.

3.2. Stress Analysis of the Top-Coal Caving Hydraulic Support

The stress analysis of the existing top-coal caving hydraulic support should be carried out to clarify the mechanical and structural characteristics of the existing support before reforming each component in a targeted manner.

The main bearing component of the top-coal caving hydraulic support is the top beam, so the top beam is used for the stress analysis. During the advancement of the working face, the load distribution on the top beam changes constantly, so the overlying load is generally simplified as a uniform load or a triangular load in the stress analysis of the hydraulic support. The work simplified the overburden load as a uniform load (Figure 5). Points A and B are the constraints of the front and rear columns on the top beam, respectively; F_1 and F_2 the support stress of the front and rear columns, respectively; f is the friction force on the top beam; q the load on the top beam; point O the front endpoint of the top beam, with a reference system established for the top beam.

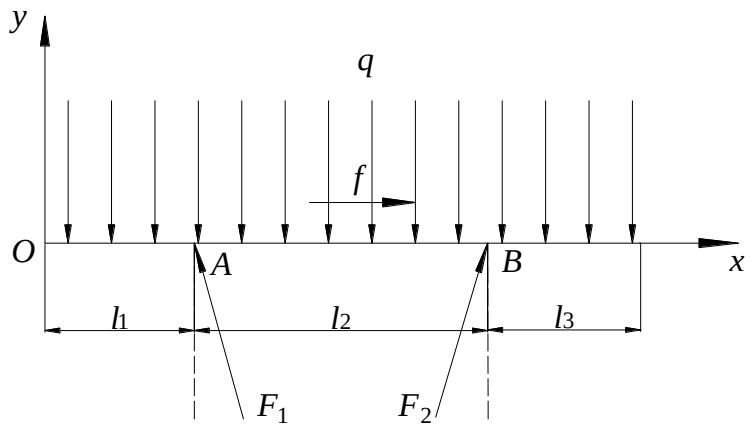


Figure 5. Mechanical model of the top beam of the top-coal caving hydraulic support.

The equation is constructed from the equilibrium state of the support.
If the resultant moment at point O is zero.

$$\begin{gathered} \sum M_o = 0 \\ \cos\alpha F_1 l_1 + \cos\beta F_2 (l_1 + l_2) - \tfrac{q}{2}(l_1 + l_2 + l_3)^2 = 0 \end{gathered} \tag{1}$$

If the resultant force in the x direction is zero.

$$\begin{gathered} \sum F_x = 0 \\ -\sin\alpha F_1 + \sin\beta F_2 + f = 0 \end{gathered} \tag{2}$$

If the resultant force in the y direction is zero.

$$\begin{gathered} \sum F_y = 0 \\ \cos\alpha F_1 + \cos\beta F_2 - q(l_1 + l_2 + l_3) = 0 \end{gathered} \tag{3}$$

The dimensions of the top beam of the ZFS5600/16/32 top-coal caving hydraulic support are as follows: l_1 = 0.5, l_2 = 0.98, l_3 = 0.51. When the support height is at 1600–3200 mm, the support state at the height of 2.5 m is taken to solve the load. Corresponding column-angle parameters are as follows: $a = 5^\circ$, $\beta = 2^\circ$. Then,

$$\begin{gathered} F_1 = 0.99q \\ F_2 = 1.01q \\ f = -0.12q \end{gathered} \tag{4}$$

The load ratio of the front and rear columns is F_1:F_2 = 0.98:1. The stress of front and rear columns is not much different under the uniform load, and the load-bearing capacity

of the rear column is 2% larger than that of the front column. The main structures such as the top beam of the top-coal caving hydraulic support can be used. Considering that the top beam needs to support the backfilling space, it is necessary to strengthen the support function of the rear column based on the top-coal caving support.

3.3. Basic Frame Parameters of the New Backfilling Hydraulic Support

Table 2 shows the basic parameters of the backfilling hydraulic support based on the geological conditions and performance requirements. The new backfilling hydraulic support adopts the form of 6-column support; the compaction mechanism adopts a single-stage telescopic box structure, and the swing is realized using the inclined-pull jack. Its model is the ZC4800/16/30 backfilling hydraulic support (Figure 6).

Table 2. Main technical parameters of ZC4800/16/30 backfilling hydraulic support.

Project	Parameter	Project	Parameter
Center distance	1500 mm	Initial support	2786 kN
Height	1600–3000 mm	Work resistance	4800 kN
Width	1420–1590 mm	Support strength	0.56 MPa

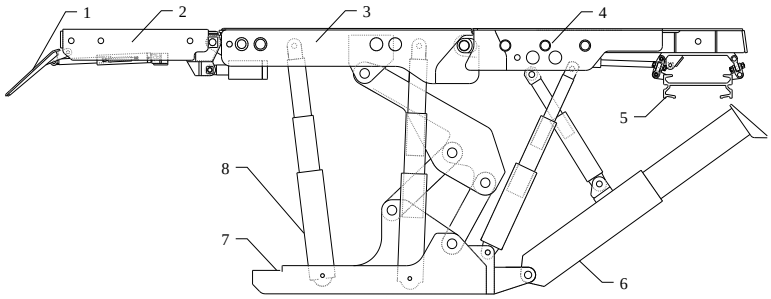


Figure 6. Floor plan of the ZC4800/16/30 backfilling hydraulic support. 1. Guard plate; 2. Front extension beam; 3. Top beam; 4. Rear top beam; 5. Perforated bottom-dump conveyor; 6. Compaction mechanism; 7. Base; 8. Column.

3.4. Renovation and Optimization of Components

According to the structural differences between the two kinds of supports and the problems existing in using the backfilling hydraulic supports, parts of the supports in the reconstruction plan are composed of reconstruction and renovation (Figure 7).

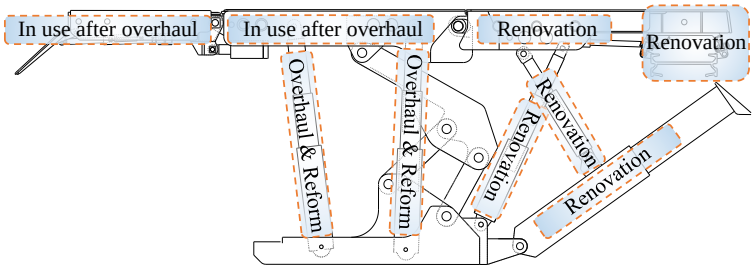


Figure 7. Reconstruction position of hydraulic supports.

4. Mechanical Analysis and Strength Check of the Backfilling Hydraulic Support

After the reconstruction and renovation, it is necessary to evaluate the rationality of the design of the backfilling hydraulic support and its performance in the application process according to the stress analysis, strength check, and backfilling operation characteristics. In this chapter, the plane model and 3D model of the backfilling hydraulic support are

established for the plane stress analysis and strength tests of the whole frame, respectively. The backfilling operation characteristics analysis is carried out in the next chapter.

4.1. Mechanical Analysis of the Backfilling Hydraulic Support

The biggest difference between the modified backfilling hydraulic support and the original top-coal caving hydraulic support is that it adds a rear top beam and increases the roof control area, which requires the stress analysis of the top beam [35]. The mechanical model is established by taking the reformed top beam of the ZC4800/16/30 backfilling hydraulic support. Points B, C, and D are the constraints of the front, middle and rear columns on the top beam, respectively; F_1, F_2, and F_3 the supporting force of the front, middle and rear columns, respectively; f is the friction force on the top beam; q the load on the top beam; point O the hinge point of the front and rear top beams (see Figure 8).

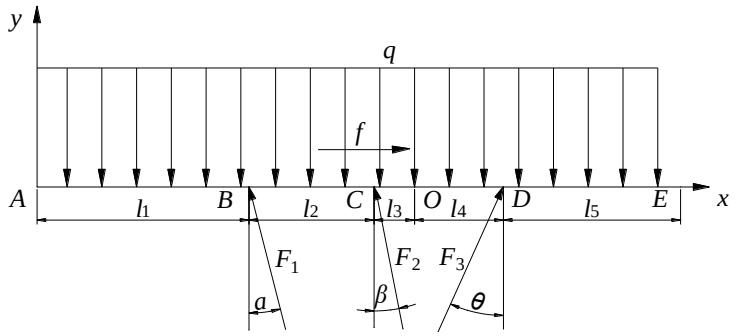


Figure 8. Backfilling hydraulic support with a uniform external load on the top beam.

The overall uniformly distributed load form of the front and rear top beams is $q(x) = q$. The equation is constructed from the support in equilibrium.

$$\begin{cases} \sum F_x = 0 & -\sin\alpha F_1 - \sin\beta F_2 + \sin\theta F_3 + f = 0 \\ \sum F_y = 0 & \cos\alpha F_1 + \cos\beta F_2 + \cos\theta F_3 - q(l_1 + l_2 + l_3 + l_4 + l_5) = 0 \\ \sum M_{o-left} = 0 & \cos\alpha F_1(l_2 + l_3) + \cos\beta F_2 l_3 - \frac{q}{2}(l_1 + l_2 + l_3)^2 = 0 \\ \sum M_{o-right} = 0 & \cos\theta F_3 l_4 - \frac{q}{2}(l_4 + l_5)^2 = 0 \end{cases} \tag{5}$$

The dimensions of the top beam of the backfilling hydraulic support are as follows: l_1 = 0.72, l_2 = 1.302, l_3 = 0.383, l_4 = 1.019, l_5 = 0.977. According to measurement data, when the support height is at 1.6–3.0 m, the angles between the front, middle, and rear columns and the vertical direction are as follows: a = 10.5~23.7°, β = 2.1~4.2°, θ = 23.6~51.1°. The support state at a height of 2.5 m is taken to solve the load ratio, and corresponding angles of columns are as follows: a = 11.6°, β = 3.4°, θ = 29.5°. Maple is used to write the corresponding calculation program.

$$\begin{aligned} F_1 &= 1.53q; \\ F_2 &= 0.95q; \\ F_3 &= 2.25q; \\ f &= -0.74q \end{aligned} \tag{6}$$

Loads of the front, middle and rear columns are F_1: F_2: F_3 = 1:0.62:1.47. At the uniform load, the stress of the rear column is the largest, followed by that of the front and middle columns. The modified hydraulic support should be manufactured with appropriate material strength combined with the stress characteristics of the front, middle and rear columns. Necessary reinforcement is required for columns bearing relatively large loads.

4.2. Strength Check of the Backfilling Hydraulic Support

In addition to checking the rationality of the plane structure of the backfilling hydraulic support by the mechanical model, it is necessary to comprehensively test the bearing strength of the whole frame under the combined action of its 3D structure and material manufacturing using the finite element analysis.

The boundary conditions of the model and the connection between the parts are shown in Figure 9. The displacement boundary conditions are applied at the front and rear of the model, and the load is applied at the top beam. The connection methods between the components include normal hinges and spherical hinges, with spherical hinges used at the columns and normal hinges used at the rest of the model.

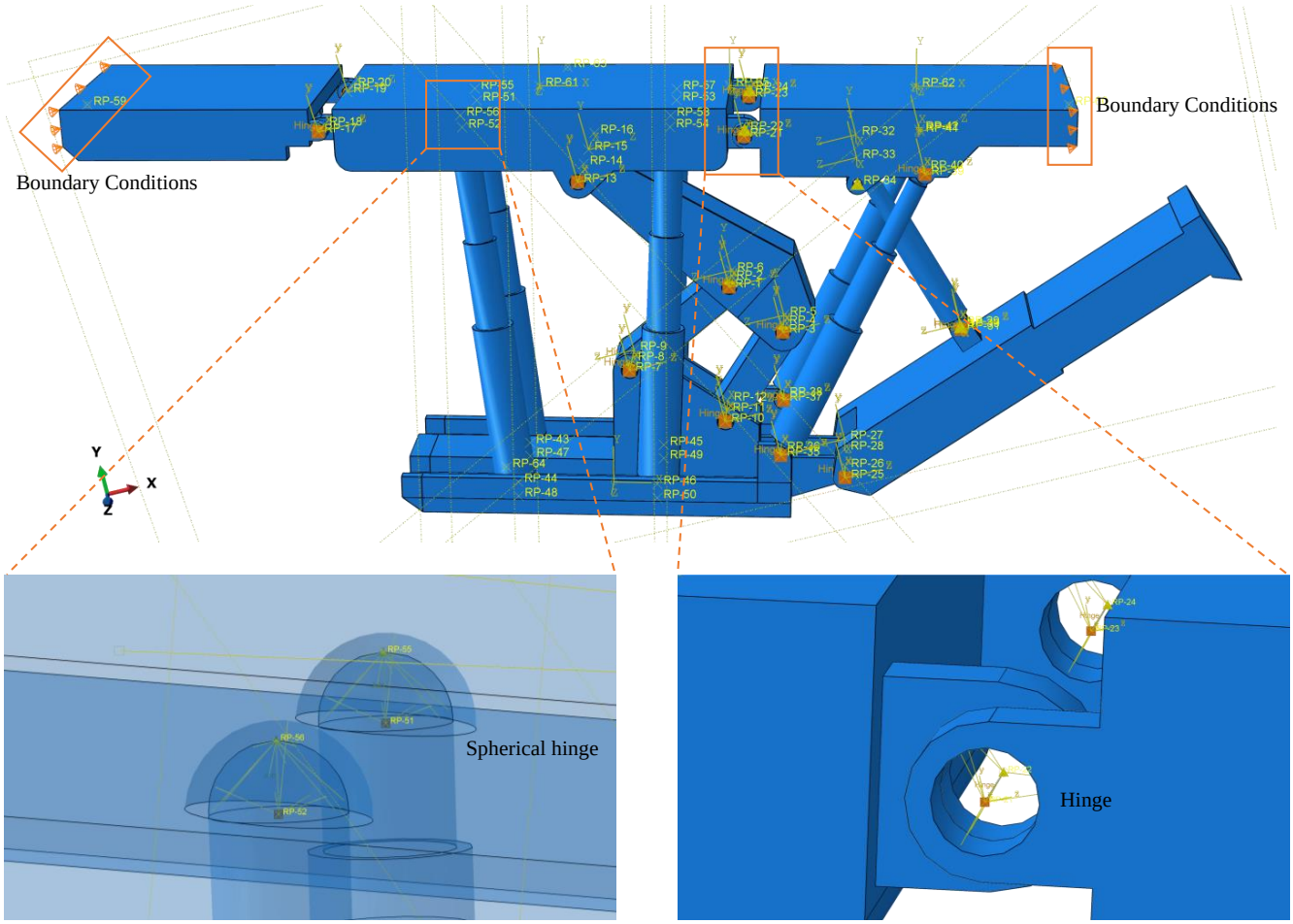


Figure 9. The boundary conditions of the model and the connection between the components.

After the pre-processing before ABAQUS modeling, a uniformly distributed load (5160 kN), 1.2 times the working resistance, is added according to the experimental theory of support strength. Figure 10 shows that the maximum stress of the whole frame is 797.8 MPa, which appears at the hinged connection between the base and the rear column. If the connection is weak, it is necessary to give Q960 steel to the connection and thicken it to ensure that it is within the allowable range of the material. The stress of other parts is within 300 MPa, and Q460 steel can be used.

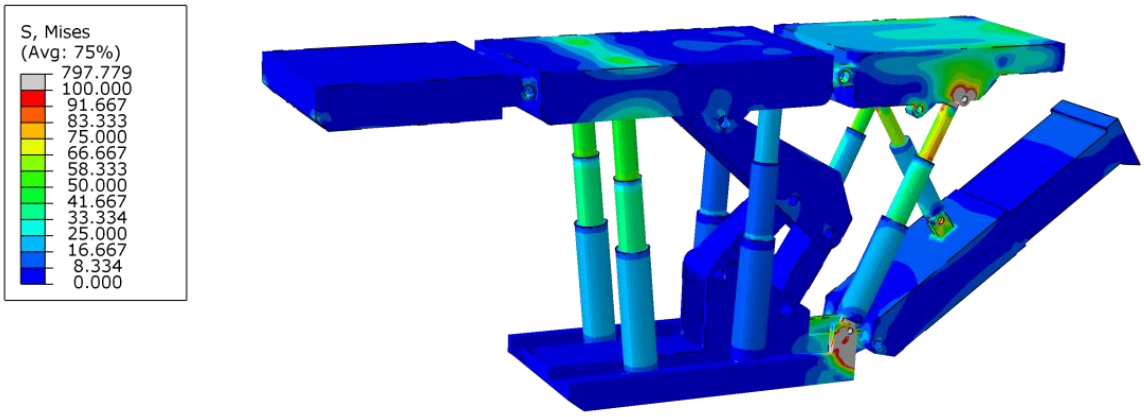


Figure 10. Stress of the whole support.

In Figure 11, the stress data of the middle node of each column are selected as a reference. The stress values of the middle nodes of the front, middle and rear columns are 22.09, 14.71, and 41.43 MPa, and the column load ratio is 1:0.67:1.64. The stress of the column is in the descending order of rear, front, and middle columns, proving that the 3D support structure with given materials is in line with the theoretical analysis results.

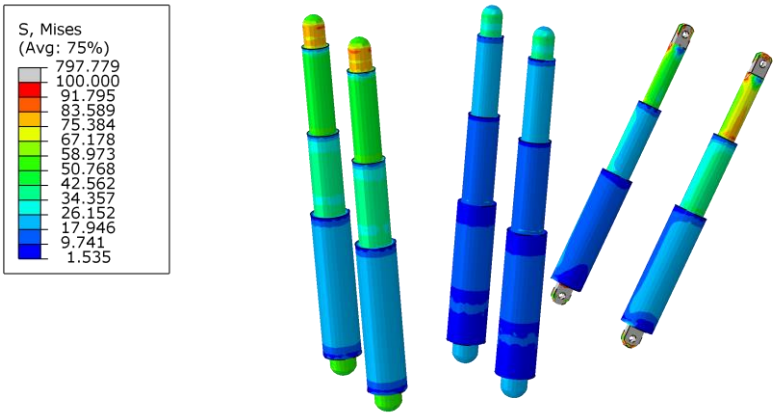


Figure 11. Stress of columns.

Figures 12–14 show the stress clouds of the top beam, the rear top beam and the base, respectively. It can be seen that the force of the top beam is mainly concentrated in the front column and the connection with other components, which is the same as the load distribution of the column. The force of the rear top beam is mainly distributed at the connection with the rear column, and the maximum can reach 610 MPa. This is because the structure is weak here, and the stress concentration occurs easily; therefore, the thickness here can be enhanced appropriately. From the stress distribution of the base, the stress is mainly concentrated in the connection between the base and the rear and front columns. Especially important, the connection between it and the rear column is prone to stress concentration; therefore, the thickness of this area should be increased.

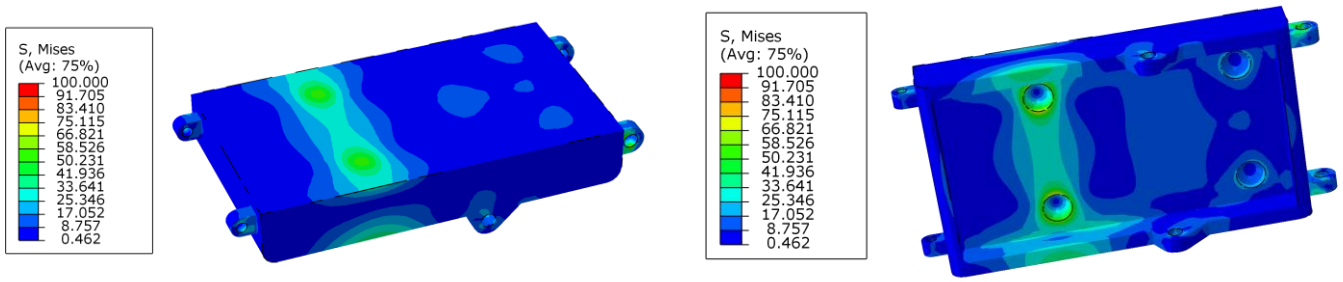


Figure 12. Stress of top beam.

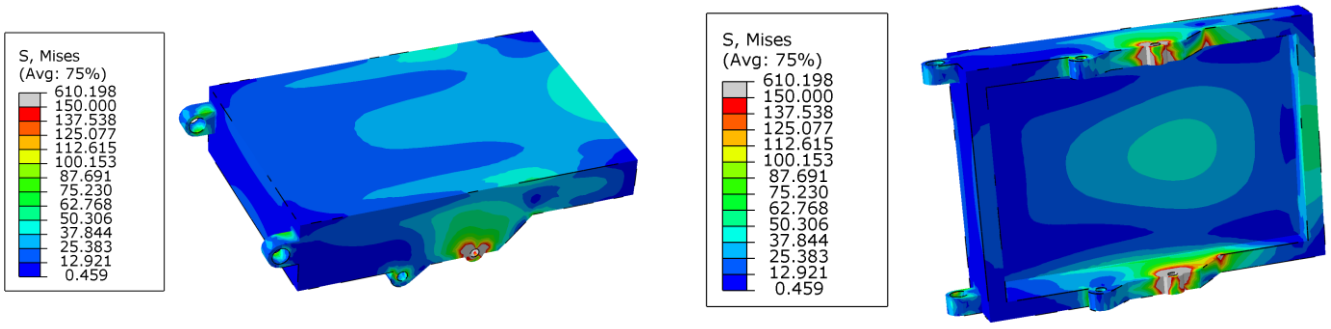


Figure 13. Stress of rear top beam.

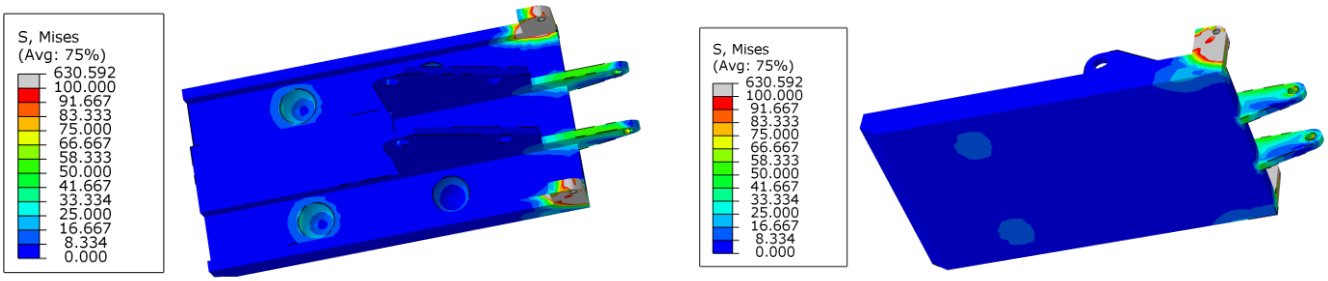


Figure 14. Stress of base.

The theoretical stress analysis of the plane structure of the backfilling hydraulic support and the finite element loading analysis of the 3D structure show that the ZC4800/16/30 backfilling hydraulic support after reformation can meet the production requirements in terms of the structure. The design is more reasonable, e.g., the strength of the whole frame within the allowable range, the stress law of each column meeting the requirements, and the sufficient support strength of the rear column.

5. Structural Analysis and Evaluation of the Backfilling Hydraulic Support

The concept of backfilling operation characteristics specifically refers to the comprehensive performance of the backfilling hydraulic support when it protects the backfilling space, provides the conveying channel and compaction power, and ensures the backfilling rate and other functions. The work performed specific characterizations from mechanical properties, structural properties, motion interference properties, strength check, compaction properties, and geological adaptation properties (see Figure 15) [36].

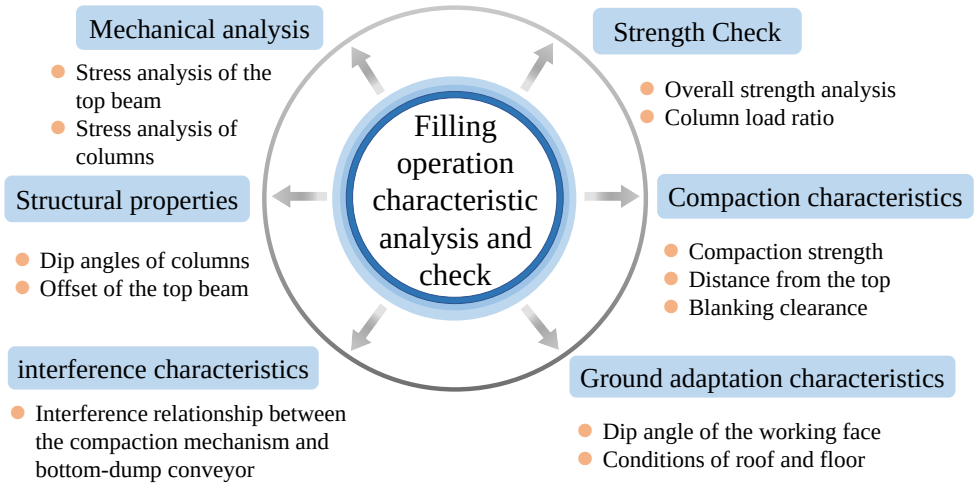


Figure 15. Backfilling characteristic indices.

In modeling software Creo 5.0(PTC. US), according to the basic parameters and structure of the ZC4800/16/30 backfilling hydraulic support, its skeleton model is established. A servo motor is introduced for motion simulation to examine the rationality of its structural design (see Figure 16 for its skeleton model).

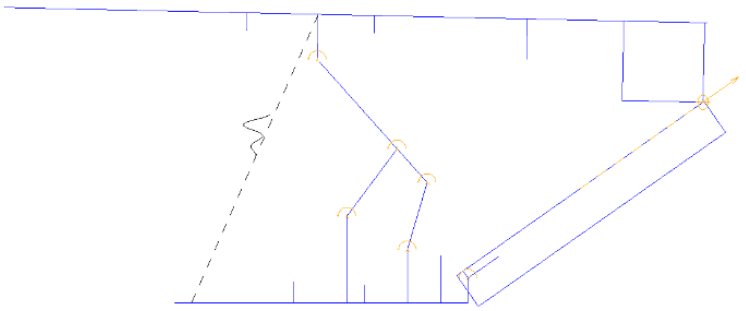


Figure 16. Skeleton of the ZC4800/16/30 backfilling hydraulic support.

5.1. Structural Characteristics

The structural characteristics of the backfilling hydraulic support refer to the basic parameters determined by the structural characteristics of the support, including the dip angle of columns and the offset of the top beam [36].

The supporting efficiency decreases with the increase in the dip angle of column, so it is necessary to check whether there is a suitable support interval. In Figure 17, the variation range of the angle between the front, middle and rear columns and the horizontal direction is 74.6–78.4°, 85.8–86.6°, and 50.8–60.5°, respectively, within the support range of 2.0–2.5 m. The middle column can convert support force to the vertical component to the greatest extent; the rear column can convert 77–87% of support force to the vertical component; the front, middle and rear columns have the high support component of the top beam. It shows that the dip angles of columns in this support interval are more reasonable.

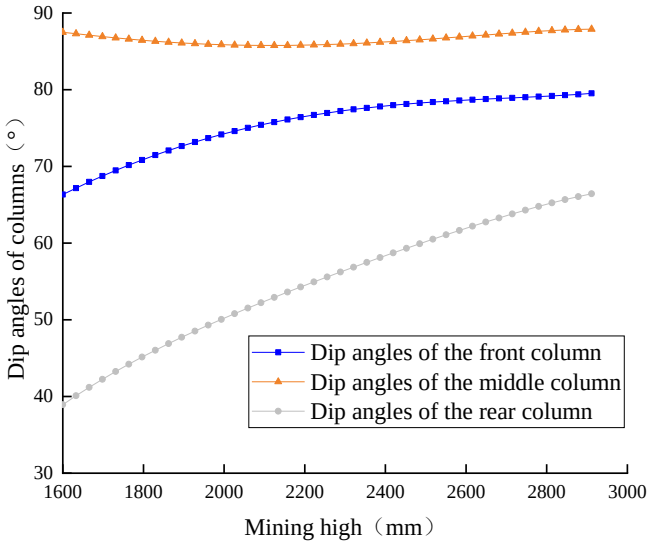


Figure 17. Variation of dip angles of columns of the ZC4800/16/30 backfilling hydraulic support.

The offset of the top beam can reflect the overall stability of the support. In Figure 18, the offset of the top beam of the ZC4800/16/30 backfilling hydraulic support first increases and then decreases, and the maximum value is 86.7 mm. It is within a reasonable deflected range of the twisted pair from the perspective of engineering.

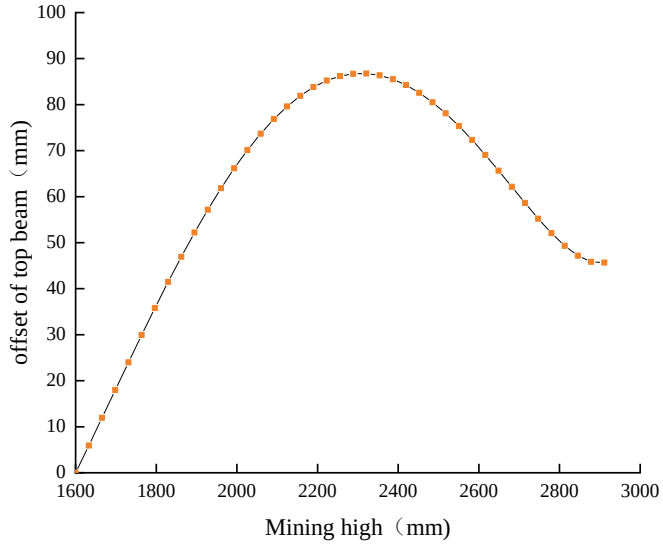


Figure 18. Variation of offset of the top beam of the ZC4800/16/30 backfilling hydraulic support.

Considering the dip angles of columns and the offset of the top beam of the ZC4800/16/30 backfilling hydraulic support, its structural characteristics meet the basic requirements.

5.2. Compaction Characteristics

The compaction characteristics of the backfilling hydraulic support refer to the basic parameters when compaction is performed using filling materials, including compaction force and angles, the distance from the top, and the blanking clearance [36].

Compaction force is the compaction pressure of the compaction mechanism on the filling material. The ZC4800/16/30 backfilling hydraulic support compaction mechanism is designed for single-stage compaction. Combined with engineering experience, the compaction mechanism should provide a compaction strength of not less than 2.5 MPa to ensure the compaction effect of the filling material.

The compaction angle refers to the angle between the compaction mechanism and the base when the compaction mechanism is extended. In Figure 19, the compaction angle of the ZC4800/16/30 backfilling hydraulic support is at 10–35°. The maximum compaction angle increases linearly with the increased mining height, and the maximum compaction angle is obtained at the maximum mining height. The compaction mechanism has a sufficient moving range for compaction materials.

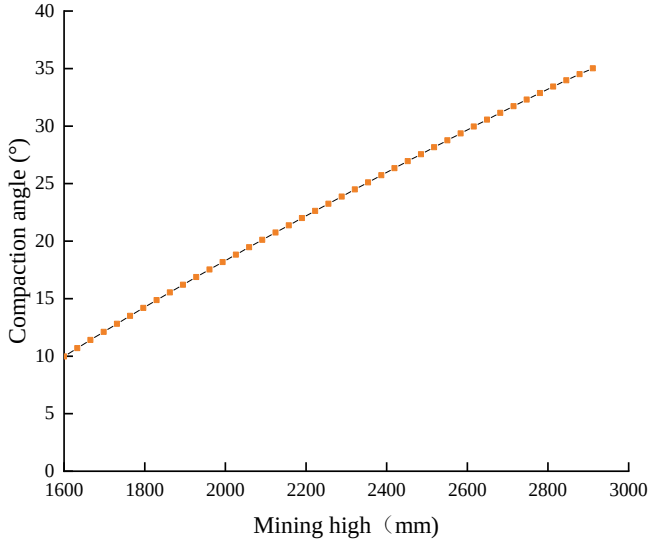


Figure 19. Compaction angle of the ZC4800/16/30 backfilling hydraulic support.

The distance from the top refers to the vertical distance between the compaction head at the front end of the compaction mechanism and the top plate after the compaction mechanism of the backfilling hydraulic support is fully extended. In Figure 20, the distance from the top changes in a smiling curve, and the bottom of the smiling curve is the most suitable working height area for the support. It roughly coincides with the mining height range of 2.0–2.5 m, indicating that the distance from the top is more reasonable. The sensitive area of the distance from the top is located on the right side of the most suitable working height area, just avoiding the influence of the change at the mining height of 2.0–2.5 m.

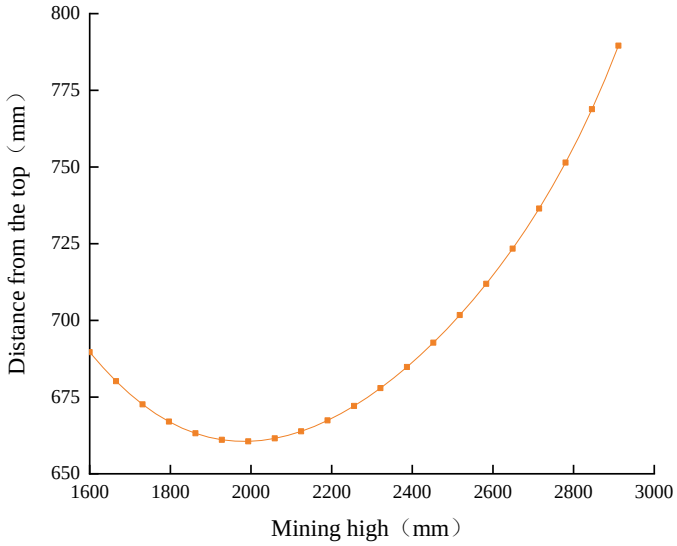


Figure 20. Variation in the distances from the top of the ZC4800/16/30 backfilling hydraulic support.

The blanking clearance affects the accumulation state of the filling material. In Figure 21, the blanking clearance of the ZC4800/16/30 backfilling hydraulic support first increases and then decreases. When the mining height is 2.0–2.5 m, the maximum blanking clearance can be obtained, that is, the maximum blanking space can be created. The rear of the stand also has enough working space at this point.

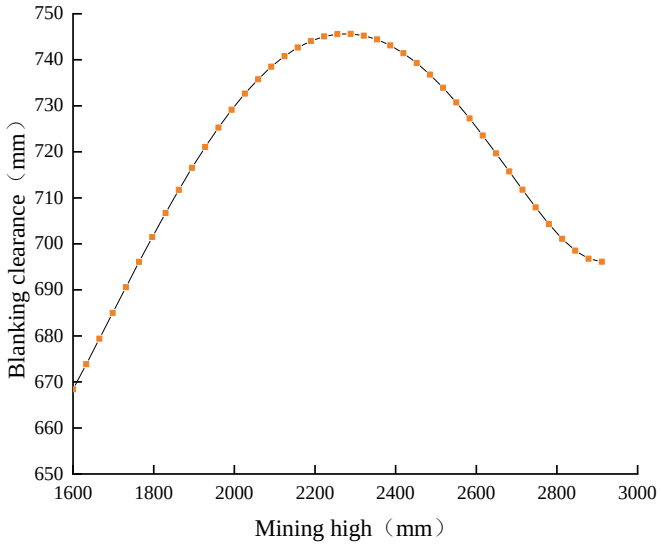


Figure 21. The change of blanking clearance of the ZC4800/16/30 backfilling hydraulic support.

Based on the compaction force, compaction angle, distance from the top, and blanking clearance of the ZC4800/16/30 backfilling hydraulic support, its compaction characteristics meet the basic requirements.

5.3. Adaptability to Geological Conditions

The adaptability of geological conditions refers to the adaptability of the backfilling hydraulic support to the geological conditions, such as the dip angle of the coal seam, the conditions of the roof and floor, the mining height, and the advanced subsidence of the roof. The six-column positive four-bar support is suitable for backfilling the coal mining working faces with small dip angles of coal seam and fine roof conditions. Therefore, the ZC4800/16/30 backfilling hydraulic support can better meet the needs of the working face of the coal seam with small dip angles.

5.4. Structural Interference Characteristics

The structural interference characteristic refers to the mutual interference effect between the compaction mechanism backfilling the hydraulic support and the porous bottom discharge conveyor. A 3D model is established in Creo to check the interference in the compaction process. The distance that the perforated bottom-dump conveyor can translate forward and backward is 680 mm, and the compaction angle of the compaction mechanism is 10–35°. Moreover, interference checks are performed at extreme positions. When the compaction angle is 10°, the distance between the compaction mechanism and the conveyor is the farthest. The conveyor can move freely without mutual interferences. In Figure 22, when the conveyor is moved to the very rear end of the top beam, the compaction angle is a maximum of 35°.

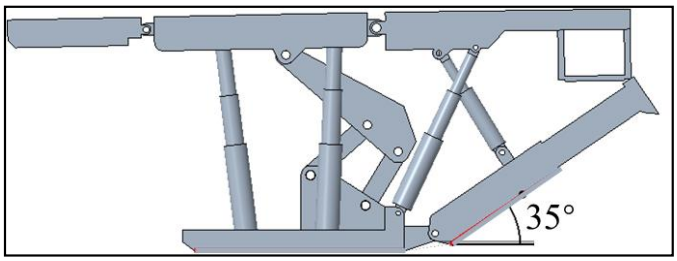


Figure 22. Critical compaction angle of the perforated bottom-dump conveyor.

In Figure 23, when the perforated bottom-dump conveyor moves to the front end of the slideway, that is, when the maximum allowable distance from the front end of the rear roof beam is 1.466 m, the compaction angle can be increased to 42° without interferences.

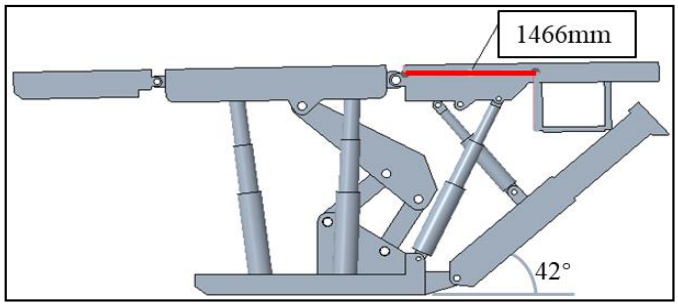


Figure 23. Critical compaction angle after moving perforated the bottom-dump conveyor.

The check structure shows that the compaction mechanism is within the range of the compaction angle, and the compaction mechanism and the perforated bottom-dump conveyor do not interfere. They can cooperate well with each other to complete the backfilling process of the working face for coal mining.

It is found that the renovated design of the ZC4800/16/30 backfilling hydraulic support meets the basic requirements by checking the structural characteristics, compaction characteristics, geological adaptation characteristics, and structural interference characteristics of the hydraulic support above.

6. Engineering Applications

The modified backfilling hydraulic supports are shown in Figure 24. The utilization rate of the old parts of the hydraulic supports in the renovation exceeded 50%, and the components of the top-coal caving hydraulic supports were utilized to the greatest extent. The mining cost per ton of coal was reduced with reduced waste and saved manufacturing costs.

The modified ZC4800/16/30 backfilling hydraulic support was used in the backfilling and mining of coal #5 (with an average thickness of 2.4 m) in a mine in Hebei. The measured analysis of two working face is shown in Figure 25. In #1 working face, the average weighting step is 12.5 m and the maximum dynamic load coefficient is 1.77. In No. 2 working face, the average weighting step is 29.6 m and the maximum dynamic load coefficient is 1.20. This means that the rock pressure at the working face supported by the backfilling hydraulic support is significantly lower than that at the collapsed working face, with a difference of 47.5%. The ramming force is just above 2.0 MPa, which meets the ramming force design requirements.



Figure 24. The modified backfilling hydraulic supports.

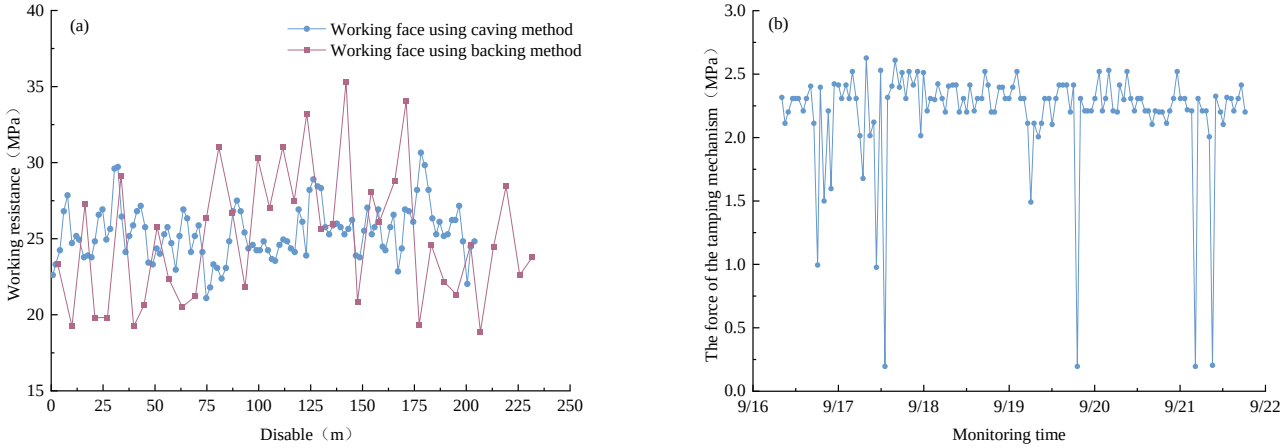


Figure 25. The measured results of backfilling hydraulic support: (**a**) Comparison of the working resistance of hydraulic supports with different mining methods; (**b**) Tamping force of backfilling hydraulic supports.

In terms of the operation of the backfilling hydraulic support, compared with the original backfilling hydraulic support during use, the initial support force of the rear column was large, and the rear top beam did not drop. Filling materials were fully dropped, which improved the filling quality. The gangue blocking plate of the compaction mechanism was high enough to reduce the probability of filling the compaction mechanism with gangue. The single-stage compaction mechanism reduced the accident rate of the elevating system, and the maintenance time was also greatly shortened. There was no major equipment operation problem during using the backfilling hydraulic support, with a good overall application effect.

The two working faces [37,38] where the hydraulic support was used for reconstructing the working face produced a total of 311,000 tons of coal resources and 405,000 tons of gangue. The mining-to-charge ratios of the two working faces were 1:1.29 and 1:1.32, respectively, and the backfilling rate reached 80%.

7. Conclusions

In this study, from the demand of accelerating the design and manufacture cycle of the backfilling hydraulic support, the abandoned top-coal caving hydraulic support is reused, the method and process of reformation are proposed, and the strength and structural

performance of the reformed backfilling hydraulic support are evaluated using numerical simulation and emulation. The main conclusions are as follows.

(1) The mechanical model of the top-coal caving hydraulic support and the backfilling hydraulic support was established to analyze its stress characteristics. The column load ratio under uniform load was 1:0.62:1.47. The stress of the rear column is the largest, followed by that of the front and middle columns. A numerical model was established using ABAQUS, and the simulated column load ratio was 1:0.67:1.64. The conclusions of theoretical analysis and numerical analysis verified the rationality of the support–structure reformation design.

(2) Creo was used to build the skeleton model of the modified hydraulic support. The structural characteristics, compaction characteristics, geological adaptation characteristics, and structural interference characteristics of the new backfilling hydraulic support were analyzed using motion simulation. The suitable support interval for backfilling hydraulic support was consistent with the mining height range, verifying that the support performance after reconstruction meets the requirements.

(3) The engineering application shows that the rock pressure at the working face supported by the backfilling hydraulic support is 47.5% lower than that at the collapsed working face. Additionally, the ramming force is just above 2.0 MPa, indicating that the support structure and performance meet the requirements. After the transformation, the utilization rate of the old parts exceeds 50%, which saves the manufacturing cost of the new backfilling hydraulic support and reduces the cost of coal mining per ton of filling and mining.

Author Contributions: Conceptualization and methodology, P.S. and Q.Z.; software and validation, P.S. and T.Z.; writing—original draft preparation, P.S. and M.L.; writing—review and editing, Q.Z. and W.S.; supervision and funding acquisition, Q.Z. All authors have read and agreed to the published version of the manuscript.

Funding: This work was supported by the National Natural Science Foundation of China General Project (Grant No. 52174134), National Natural Science Foundation of China Youth Science Foundation Project (Grant No. 51904110), and Fundamental Research Funds for Central Universities (Grant No. 2021GJZPY12).

Institutional Review Board Statement: Not applicable.

Informed Consent Statement: Not applicable.

Data Availability Statement: The data presented in this study are available on request from the corresponding author.

Acknowledgments: Thanks to Tangshan coal mine for the parameters of the hydraulic support and thank Hongjun Liu and Xiuguo Tian for their on-site guidance.

Conflicts of Interest: The authors declare no conflict of interest.

References

1. Behera, S.K.; Mishra, D.P.; Singh, P.; Mishra, K.; Mandal, S.K.; Ghosh, C.N.; Kumar, R.; Mandal, P.K. Utilization of Mill Tailings, Fly Ash and Slag as Mine Paste Backfill Material: Review and Future Perspective. *Constr. Build. Mater.* **2021**, *309*, 125120. [CrossRef]
2. Li, J.; Yilmaz, E.; Cao, S. Influence of Industrial Solid Waste as Filling Material on Mechanical and Microstructural Characteristics of Cementitious Backfills. *Constr. Build. Mater.* **2021**, *299*, 124288. [CrossRef]
3. Ma, F.; Zhao, H.; Yuan, R.; Guo, J. Ground Movement Resulting from Underground Backfill Mining in a Nickel Mine (Gansu Province, China). *Nat. Hazards* **2015**, *77*, 1475–1490. [CrossRef]
4. Huang, Y.; Wang, J.; Li, J.; Lu, M.; Guo, Y.; Wu, L.; Wang, Q. Ecological and Environmental Damage Assessment of Water Resources Protection Mining in the Mining Area of Western China. *Ecol. Indic.* **2022**, *139*, 108938. [CrossRef]
5. Li, J.; Huang, Y.; Ouyang, S.; Guo, Y.; Gao, H.; Wu, L.; Shi, Y.; Zhu, L. Transparent Characterization and Quantitative Analysis of Broken Gangue's 3D Fabric under the Bearing Compression. *Int. J. Min. Sci. Technol.* **2022**, *32*, 335–345. [CrossRef]
6. Pomykała, R.; Kępys, W. The Properties of the Backfill Mixtures Based on Own Fine-Grained Waste. In *Minefill 2020–2021, Proceedings of the 13th International Symposium on Mining with Backfill, Katowice, Poland, 25–28 May 2021*; CRC Press-Balkema: Leiden, The Netherlands, 2021; pp. 102–107.

7. Li, H.; Guo, G.; Zhai, S. Mining Scheme Design for Super-High Water Backfill Strip Mining under Buildings: A Chinese Case Study. *Environ. Earth Sci.* **2016**, *75*, 1017. [CrossRef]
8. Niroshan, N.; Yin, L.; Sivakugan, N.; Veenstra, R.L. Relevance of SEM to Long-Term Mechanical Properties of Cemented Paste Backfill. *Geotech. Geol. Eng.* **2018**, *36*, 2171–2187. [CrossRef]
9. Yilmaz, E.; Belem, T.; Benzaazoua, M. Effects of Curing and Stress Conditions on Hydromechanical, Geotechnical and Geochemical Properties of Cemented Paste Backfill. *Eng. Geol.* **2014**, *168*, 23–37. [CrossRef]
10. Al-Moselly, Z.; Fall, M.; Haruna, S. Further Insight into the Strength Development of Cemented Paste Backfill Materials Containing Polycarboxylate Ether-Based Superplasticizer. *J. Build. Eng.* **2022**, *47*, 103859. [CrossRef]
11. Sivakugan, N.; Veenstra, R.; Naguleswaran, N. Underground Mine Backfilling in Australia Using Paste Fills and Hydraulic Fills. *Int. J. Geosynth. Ground Eng.* **2015**, *1*, 18. [CrossRef]
12. Yin, W.; Chen, Z.; Quan, K.; Mei, X. Strata Behavior at Fully-Mechanized Coal Mining and Solid Backfilling Face. *SpringerPlus* **2016**, *5*, 1611. [CrossRef] [PubMed]
13. Yu, M.; Wu, M.; Yang, X.; Lou, R.; Wang, F.; Li, H.; Wang, L. Effect of Temperature on the Evolution and Distribution for Particle Size of Loose Broken Coal during the Uniaxial Confined Compression Process. *Fuel* **2022**, *318*, 123592. [CrossRef]
14. Ermolovich, E.A.; Ivannikov, A.L.; Khayrutdinov, M.M.; Kongar-Syuryun, C.B.; Tyulyaeva, Y.S. Creation of a Nanomodified Backfill Based on the Waste from Enrichment of Water-Soluble Ores. *Materials* **2022**, *15*, 3689. [CrossRef] [PubMed]
15. Khayrutdinov, A.M.; Kongar-Syuryun, C.B.; Kowalik, T.; Tyulyaeva, Y.S. Stress-Strain Behavior Control in Rock Mass Using Different-Strength Backfill. *MIAB. Mining Inf. Anal. Bull.* **2020**, *10*, 42–55. [CrossRef]
16. Cavusoglu, I.; Yilmaz, E.; Yilmaz, A.O. Sodium Silicate Effect on Setting Properties, Strength Behavior and Microstructure of Cemented Coal Fly Ash Backfill. *Powder Technol.* **2021**, *384*, 17–28. [CrossRef]
17. Cihangir, F.; Akyol, Y. Effect of Desliming of Tailings on the Fresh and Hardened Properties of Paste Backfill Made from Alkali-Activated Slag. *Adv. Mater. Sci. Eng.* **2020**, *2020*, 4536257. [CrossRef]
18. Bywalski, C.; Drzazga, M.; Kaźmierowski, M.; Kamiński, M. Shear Behavior of Concrete Beams Reinforced with a New Type of Glass Fiber Reinforced Polymer Reinforcement: Experimental Study. *Materials* **2020**, *13*, 1159. [CrossRef]
19. Behera, S.K.; Ghosh, C.N.; Mishra, D.P.; Singh, P.; Mishra, K.; Buragohain, J.; Mandal, P.K. Strength Development and Microstructural Investigation of Lead-Zinc Mill Tailings Based Paste Backfill with Fly Ash as Alternative Binder. *Cem. Concr. Compos.* **2020**, *109*, 103553. [CrossRef]
20. Behera, S.K.; Mishra, D.P.; Ghosh, C.N.; Prashant; Mandal, P.K.; Singh, K.M.P.; Buragohain, J.; Singh, P.K. Strength and Micro-Structure Evolution of Compacted Soils Modified by Admixtures of Cement and Metakaolin. *Appl. Clay Sci.* **2016**, *127–128*, 44–51. [CrossRef]
21. Panchal, S.; Deb, D.; Sreenivas, T. Mill Tailings Based Composites as Paste Backfill in Mines of U-Bearing Dolomitic Limestone Ore. *J. Rock Mech. Geotech. Eng.* **2018**, *10*, 310–322. [CrossRef]
22. Li, J.; Huang, Y.; Chen, Z.; Zhang, J.; Jiang, H.; Zhang, Y. Characterizations of Macroscopic Deformation and Particle Crushing of Crushed Gangue Particle Material under Cyclic Loading: In Solid Backfilling Coal Mining. *Powder Technol.* **2019**, *343*, 159–169. [CrossRef]
23. Deb, D.; Sreenivas, T.; Dey, G.K.; Panchal, S. Paste Backfill Technology: Essential Characteristics and Assessment of Its Application for Mill Rejects of Uranium Ores. *Trans. Indian Inst. Met.* **2017**, *70*, 487–495. [CrossRef]
24. Libos, I.L.S.; Cui, L. Time- and Temperature-Dependence of Compressive and Tensile Behaviors of Polypropylene Fiber-Reinforced Cemented Paste Backfill. *Front. Struct. Civ. Eng.* **2021**, *15*, 1025–1037. [CrossRef]
25. Chen, L.; Li, J.; Zhang, D.; Fan, G.; Zhang, W.; Guo, Y. Microscopic Fabric Evolution and Macroscopic Deformation Response of Gangue Solid Waste Filler Considering Block Shape under Different Confining Pressures. *Sci. Rep.* **2022**, *12*, 7388. [CrossRef] [PubMed]
26. Zhang, Q.; Zhang, J.; Kang, T.; Sun, Q.; Li, W. Mining Pressure Monitoring and Analysis in Fully Mechanized Backfilling Coal Mining Face—A Case Study in Zhai Zhen Coal Mine. *J. Cent. South Univ.* **2015**, *22*, 1965–1972. [CrossRef]
27. Zhang, Y.; Cao, J.; Jiang, L.; Liu, P.; Gui, X.; Yang, J. Simulation Research on Hydraulic Support Based Virtual Prototyping. In *Proceedings of the 9th China-Russia Symposium Coal in the 21st Century: Mining, Intelligent Equipment and Environment Protection*; Tan, Y., Chen, S., Eds.; Atlantis Press: Paris, France, 2018; Volume 176, pp. 173–179.
28. Podkolzin, A.A. Improving the Quality of Hydraulic Powered Roof Support. *Proc. Tula States Univ.-Sci. Earth* **2016**, *4*, 215–221.
29. Lu, J.; Wang, L.; Fang, Q.; Hu, J.; Liu, F.; Yang, W. Method of Structural Reliability Approximation Analysis Based on Neural Network for Structural Optimization of Hydraulic Support. In Proceedings of the 2015 Advanced Design Concepts and Practice (ADCP 2015), Hangzhou, China, 18–20 September 2015; Destech Publications, Inc.: Lancaster, UK, 2016; pp. 251–256.
30. Yang, Y.; Zeng, Q. Impact-Slip Experiments and Systematic Study of Coal Gangue "Category" Recognition Technology Part I: Impact-Slip Experiments between Coal Gangue Mixture and Top Coal Caving Hydraulic Support and the Study of Coal Gangue "Category" Recognition Technology. *Powder Technol.* **2021**, *392*, 224–240. [CrossRef]
31. Li, A.; Zheng, X.; Wang, W. Motion Simulation of Hydraulic Support Based on Unity 3D. In Proceedings of the First International Conference on Information Sciences, Machinery, Materials and Energy (ICISMME 2015), Chongqing, China, 11–13 April 2015; Ching, X., Dvorik, V., Eds.; Atlantis Press: Paris, France, 2015; Volume 126, pp. 623–626.
32. Kunyu, X.; Tong, X.; Chengming, S.; Peng, Z.; Fei, M. Research Progress on Failure Analysis and Life Assessment of Key Components in Hydraulic Supports. *China Surf. Eng.* **2022**, *35*, 97–106. [CrossRef]

33. Xie, J.; Wang, X.; Yang, Z.; Hao, S. Virtual Monitoring Method for Hydraulic Supports Based on Digital Twin Theory. *Min. Technol.* **2019**, *128*, 77–87. [CrossRef]
34. Xie, J.; Wang, X.; Yang, Z.; Hao, S. Attitude-Aware Method for Hydraulic Support Groups in a Virtual Reality Environment. *Proc. Inst. Mech. Eng. Part C J. Mech. Eng. Sci.* **2019**, *233*, 4805–4818. [CrossRef]
35. Bo, G. Stress analysis and kinematics simulation analysis of filling hydraulic support. *Coal Chem. Ind.* **2019**, *42*, 75–77+81. (In Chinese) [CrossRef]
36. Qiang, Z.; Jixiong, Z.; Yang, T.; Feng, J.; Qiang, S. The theoretical research on basic characteristics of backfilling hydraulic support and its application. *J. Min. Saf. Eng.* **2014**, *31*, 845–851. (In Chinese) [CrossRef]
37. Baojie, Y. Study on width optimization of gangue filling working face in Tangshan Mine. *China Min. Mag.* **2022**, *31*, 111–116. (In Chinese)
38. Chengxiang, F. Research on surface subsidence in mining with solid filling under buildings in coal mine. *Mine Surv.* **2021**, *49*, 27–30. (In Chinese)

Disclaimer/Publisher's Note: The statements, opinions and data contained in all publications are solely those of the individual author(s) and contributor(s) and not of MDPI and/or the editor(s). MDPI and/or the editor(s) disclaim responsibility for any injury to people or property resulting from any ideas, methods, instructions or products referred to in the content.